Materials Science-Poland, Vol. 28, No. 1, 2010

Influence of sol-gel matrices on the optical excitation of europium ions

M. BANSKI*, A. PODHORODECKI, J. MISIEWICZ

Institute of Physics, Wrocław University of Technology,
Wybrzeże Wyspiańskiego 27, 50-370 Wrocław, Poland

Photoluminescence (PL), total photoluminescence excitation (TPLE), transmission and decay photoluminescence experiments were done to establish the most efficient excitation mechanism of the europium (Eu^{3+}) ions in amorphous Al_2O_3 and $Y_3Al_5O_{12}$ host matrices. Both matrices were fabricated using the sol-gel technique, doped with Eu^{3+} ions and sputtered on a flat quartz plate. Because of relatively low temperatures of annealing (200 °C), after this treatment the matrices should remain in an amorphous phase. In such a system, Eu^{3+} ions occupy the points having different site symmetries. However, based on characteristic features of the PL spectra, the effective site symmetry (ESS) parameter was defined to describe the PL properties of the Eu^{3+} ions in various matrices. Low intensive direct f-f transitions at 392, 465, 530 nm were observed in the TPLE spectra. The most intensive, wide excitation bands were centred at around 250–260 nm and the charge transfer process was found to be related to these excitation bands. Finally, a good correlation between photoluminescence lifetimes, the PL intensity and CT energy was observed.

Keywords: *excitation mechanism; charge transfer; europium; amorphous matrix; photoluminescence*

1. Introduction

Nowadays, one of the leading research areas is the investigation of new light sources with high emission efficiency, low power consumption, stability in various environments, characterised with simple method of fabrication and low production costs.

In the last two decades, intensive investigations were performed with sol-gel materials as potential host matrices for the optically active centres [10]. One of its most important advantages of the sol-gel technology is the low cost. Another one is simplicity and the possibility of easily incorporating optical active centres (i.e., rare earth ions) [2] into sol-gel and later depositing them onto various substrates (including porous materials) [3]. It is well know that PL efficiency of rare earth (RE) ions increases

---

*Corresponding author, e-mail: mateusz.banski@pwr.wroc.pl with increasing non-centrosymmetricity of host crystals. In practice, a big challenge is to find a combination of substrate, matrix and RE ions such that photoluminescence emission is enhanced.

The advantage of RE ions is luminescence being related to the internal 4f orbital transitions. The screening of the internal 4f orbitals from the external environment by the 5d orbital electrons provides the stability of the emission wavelength in various external conditions. In addition, the emissions of different RE ions cover almost all visible range of wavelengths. As a result, RE ions have already been found to have many applications, e.g. in large-scale display screens, television sets, lasers and amplifiers [4]. However, 4f–4f transitions are in principle electric dipole forbidden according to Laporte's rule, thus the RE ions have very small absorption cross sections, which limits their use in photo-activated systems [5]. Because of this limitation, in practical applications RE ions have to be doped in a host material which plays the role of a sensitizer and increases the RE excitation efficiency.

The main role of the matrix is to increase the efficiency of RE ion photoexcitation leading to the increase of the PL intensity from the ions. The PL intensity increases, because the crystal field slightly influences the 4f orbitals of RE which overlap and cause that forbidden electric dipole transitions become allowed. Thus, Laporte's rule no longer applies in the presence of the lattice. Simultaneously, the number of the possible excitation mechanisms increases. For RE ions in the host matrix, there are four various excitation mechanisms: direct excitation of the RE ions through 4f–4f and 4f–5d transitions, and excitation through the matrix by charge transfer (CT), or energy transfer (ET). However, depending on the matrix properties (absorption coefficient, refractive index, RE ion site symmetry, etc.), different excitation mechanisms can dominate. Thus, the determination of this mechanism is crucial from the point of view of excitation/emission optimization.

From the application point of view, we expected that the ideal host material would be transparent for the visible light, environmentally stable and not fragile. Only if all these criteria are satisfied, the proposed solution will have a viable chance of becoming a commercially available product.

$Y_3Al_5O_{12}$ matrices in a crystalline form are already known to be excellent scintillators. The phosphors based on this material are widely used in cathode ray tubes, and field emission display technologies because of their optical emission intensity and long lifetime [6]. Besides the good environmental stability and high electrical resistivity, the main advantage of the Al_2O_3 matrix is its ability to incorporate a high concentration of RE ions without clustering. This phenomenon is related to the cubic crystal structure of the γ-Al_2O_3 which is very similar to the RE_2O_3 structure. This matrix can significantly enhance the RE^{3+} fluorescence [7].

$Y_3Al_5O_{12}$ and Al_2O_3 matrices were prepared using the sol-gel technique [8]. Both of them were doped with Eu^{3+} ions and sputtered on flat quartz plates. In order to reduce the cost of the production, the samples were annealed at relatively low temperatures and thus they remained in the amorphous phase.

Better information about the most efficient excitation mode will be crucial to produce more efficient and low power consuming devices. Thus, the aim of this work was to investigate the influence of an amorphous sol-gel matrix, fabricated at low temperature, on the excitation mechanism of Eu^{3+} ions. The results of the photoluminescence (PL), the total photoluminescence excitation (TPLE), as well as the transmittance measurements and PL decay have been presented.

2. Experimental

In the experiment, two samples were investigated. They were prepared using different sol-gel compounds as the matrix material, i.e. Al_2O_3, $Y_3Al_5O_{12}$ (YAG). To obtain sol-gel matrices doped with europium ions, the following compositions were used: $Al_2O_3:Eu^{3+}$ (30 wt. % of Eu_2O_3, 70 wt. % Al_2O_3), $YAG:Eu^{3+}$ ($Eu_{0,15}Y_{2,85}Al_5O_{12}$). The exact preparation procedure has already been described elsewhere [8, 9]. The sol-gel derived xerogel films (matrices) were fabricated by spin-on deposition at the rate of 2700 rpm onto flat quartz substrates, followed by drying at 200 °C for 30 min [10, 11]. Finally all the just-prepared samples were heated at 200 °C.

The experimental setup consisted of a 450 W Xenon lamp, Jobin Yvon TRIAX 180 monochromator, OceanOptics HR4000 CCD detector. The incident light, in the range from 210 to 500 nm, coming from a monochromator, was focused on the sample. The photoluminescence signal was collected and transmitted with the fibre optic device to the CCD detector. The setup for transmission measurements were based on a broadband light source – a deuterium tungsten halogen lamp. The luminescence lifetimes were measured with the equipment made by the Photon International Instruments, where the flash halogen lamp was used as a pulse source. The wavelength of the incident light was chosen by the monochromator. The second monochromator dispersed the signal recorded by a photomultiplier tube. All the measurements were done at room temperature.

3. Results and discussion

Figure 1 shows PL spectra of $Al_2O_3:Eu^{3+}$ and $Y_3Al_5O_{12}:Eu^{3+}$ samples excited with the wavelength in the maximum of the excitation band. The recorded spectrum exhibits features characteristic of the RE ion 4f–4f intrashell transitions. Four emission bands related to transition from the lowest excited state ($^5D_0$) to the ground state ($^7F_1$, $^7F_2$, $^7F_3$ and $^7F_4$) are clearly resolved at the 593, 613, 650 and 701 nm, respectively. The $^5D_0$–$^7F_2$ transition gives the most intensive emission peak in the spectrum, because it is the most probable transition as it is the electric dipole transition [12]. Luminescence from the higher excited states such as $^5D_1$ is not observed at all, indicating very efficient non-radiative (multiphonon) relaxation to the $^5D_0$ level [13]. The most intensive Eu-related photoluminescence is found for the $Y_3Al_5O_{12}$ matrix. At this point, a question arises which factors influence the emission. The understanding of these factors enables us to control the excitation properties of the Eu^{3+} ions in a sol-gel matrix.

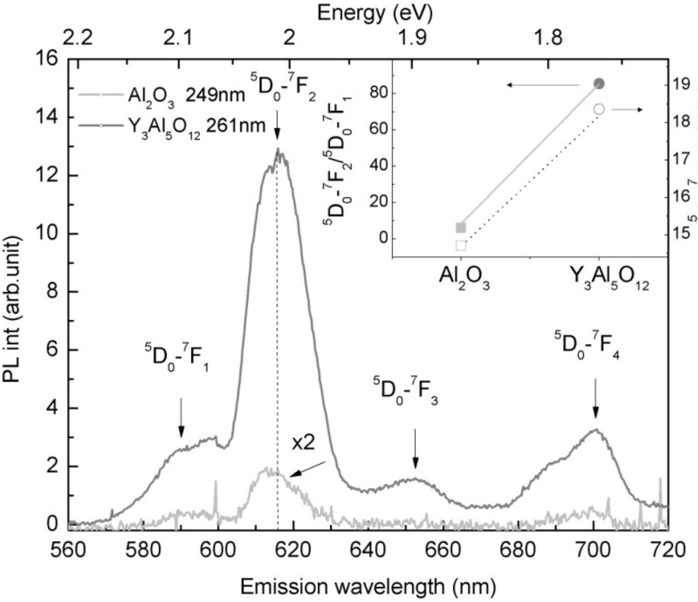

Fig. 1. The PL spectra of various sol-gel matrices doped by Eu^{3+} on the quartz substrate excited at the maximum of the excitation band. The inset shows the intensity ratio of the $^5D_0 \rightarrow {}^7F_2$ and $^5D_0 \rightarrow {}^7F_1$ and FWHM of $^5D_0 \rightarrow {}^7F_2$ transition

The emission efficiency of the RE ions depends on four factors, if they are excited non resonantly: absorption of the matrix, excitation energy transfer, emission properties of the ions and relaxation within an ion. First, the emission properties of the RE ions in two different matrices based on aluminum oxide is presented. Like the absorption, the first order emission among 4f orbitals is also forbidden by electric dipoles but it is allowed by the electric quadrupole, vibronic, magnetic dipole and forced electric dipole mechanisms. However, only the last two cases can be related to the observed emission intensities. From the experimental point of view, it was found that the emission efficiency of the ion itself depends strongly on the local symmetry of the ion site, and also on the energy difference between the excited 4f configuration and the $4f^{n-1}5d$ or CT state.

The crystal field of the host material influences not only the emission intensity from RE ions, but it also splits their ground energy levels. Because of that, few separate lines related to different transition could be observed and their number depends on the symmetry of the ion site in the matrix. In a less centrosymmetric system, the crystal lattice causes the energy levels of Eu^{3+} ions to split into a higher number of sublevels and the breadth of the emission peak increases [12]. However, in our PL spectra it is impossible to distinguish these separate lines. They are observed as one peak at around 612.5 and 615.9 nm, with the FWHM parameter equal to 14.7 and 18.4 nm for Al_2O_3 and $Y_3Al_5O_{12}$ matrices, respectively. The observed inhomogeneous broadening is due to many site symmetries of the crystal structure, which can be occupied by the Eu^{3+} ions in an amorphous matrix, and it can be additionally enhanced by the lattice defects and contamination of the hydrous species. This is characteristic of the sol-gel structures annealed at low temperatures. They are like a disordered structure with a wide inhomogeneous broadening, like in glass [14].

As was already mentioned, in the amorphous phase it is impossible to determine the site symmetry of the Eu^{3+} incorporated into the matrix. However, the measured PL spectra exhibit different properties of the Eu^{3+} ions incorporated into various matrices. This fact allows us to determine the effective site symmetry (ESS) parameter, which describes not exactly the site symmetry of the ions in the crystal structure, but rather the response of the Eu^{3+} ions to the influence of average crystal field.

To determine the order of ESS of the Eu^{3+} incorporated into various matrices, the intensity ratio $I_2(^5D_0 \rightarrow {}^7F_2)/I_1(^5D_0 \rightarrow {}^7F_1)$ which serves as an effective spectroscopic probe could be used. The sensitivity of the intensity transition ratio (I_2/I_1) arises from the fact that the $^5D_0 \rightarrow {}^7F_1$ transition is mainly magnetically allowed (i.e., it is a magnetic-dipole transition) and is independent of the site symmetry at which any Eu^{3+} ion is situated [15], while the $^5D_0 \rightarrow {}^7F_2$ transition is a hypersensitive, forced electric-dipole transition which can occur only at low symmetries with no inversion centre [14]. Thus, the higher the I_2/I_1 ratio, the lower the effective site symmetry (ESS = I_1/I_2) [16]. In our case, the intensity ratio I_2/I_1 increases and thus the ESS decreases from Al_2O_3 to $Y_3Al_5O_{12}$ (inset of Fig. 1).

In addition, the information about centrosymmetry features of the matrices can be deduced also from FHWM parameters of the $^5D_0 \rightarrow {}^7F_2$ transition (inset of Fig. 1). The obtained results indicate that inhomogeneous broadening increase from Al_2O_3 to $Y_3Al_5O_{12}$, so the ESS at which the Eu^{3+} ions are incorporated into the matrices has to decrease. It is in the good agreement with our previous result.

To deeper analyze the excitation properties of Eu^{3+} ions embedded in the matrix, the total photoluminescence excitation (TPLE) map was measured and the results are shown in Fig. 2. Figure 2a shows the 2D map of PL intensity for the $Y_3Al_5O_{12}:Eu^{3+}$ sample in function of both, the excitation and the emission wavelength. The $^5D_0 \rightarrow {}^7F_1$, $^5D_0 \rightarrow {}^7F_2$, $^5D_0 \rightarrow {}^7F_3$, $^5D_0 \rightarrow {}^7F_4$, optical transitions are well resolved and the most efficient excitation wavelength is indicated. The PLE spectra recorded for the most intensive $^5D_0 \rightarrow {}^7F_2$ transitions of Eu^{3+} in the Al_2O_3, $Y_3Al_5O_{12}$ matrices are plotted in Fig. 2b. The analysis of those spectra allows us to confirm or reject the suggestion that the sol-gel matrix is responsible for the efficient excitation of Eu^{3+} ions since obtained maxima vary with material of the matrix in which the Eu^{3+} ions are doped. Nevertheless, coming from a longer wavelength, there is a very weak absorption band (530 nm) at the PLE spectra of all the samples, related to direct excitation of europium ions by f–f transition. At 465 nm there is another optical transition related to direct excitation of Eu^{3+} on the first excited term $^7F_0 \rightarrow {}^5D_2$. The excitation on the upper term $^7F_0 \rightarrow {}^5L_6$ takes place for the photons with 392 nm wavelength [16]. However, the main excitation peaks for $A_{l2}O_3$ and $Y_3Al_5O_{12}$ are at 249 and 261 nm, respectively.

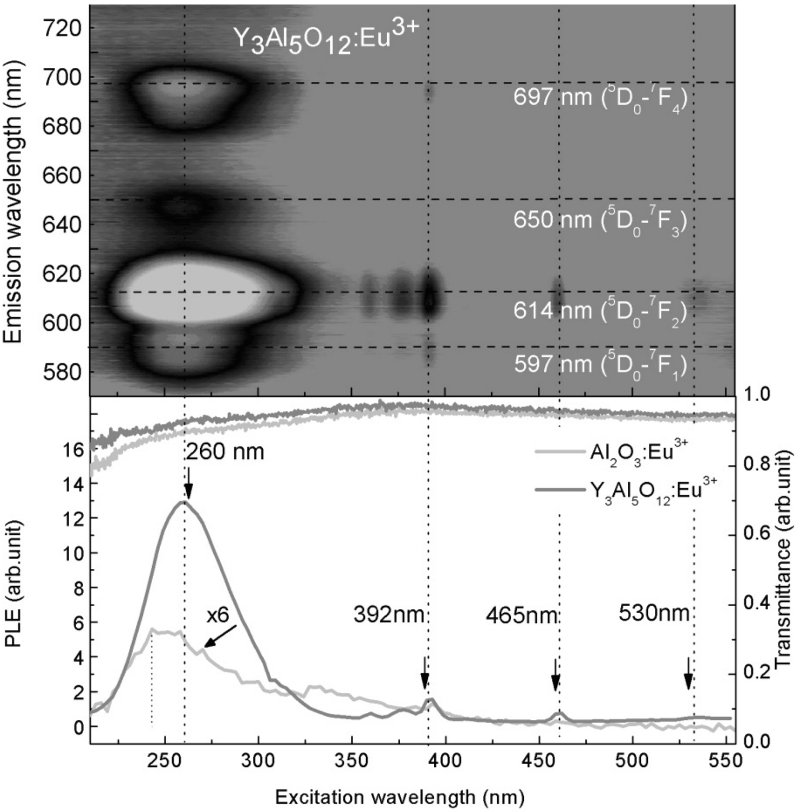

Fig. 2. TPLE map of the $Y_3Al_5O_{12}$:Eu^{3+} on a quartz plate (a), and the PLE and transmittance spectra of Al_2O_3, $Y_3Al_5O_{12}$ matrices doped by Eu^{3+} on quartz

To analyze the influence of the energy transfer (ET) on the Eu^{3+} excitation, transmission spectra have been collected for both samples. The transmission experiment gives an effective matrix response, and at low Eu^{3+} concentration it is not possible to acquire any information about the Eu^{3+} absorption properties. For the samples fabricated with Al_2O_3 and $Y_3Al_5O_{12}$ matrices, results presented in Fig. 2b confirm that those materials have a high energy gap (*Eg*) and the light almost does not interact with these matrices in the investigated wavelength range. The transmittance of such structures is over 80% even for the photons of energy 6.0 eV, as the energy gaps equal 6.6 eV for Al_2O_3 [18] and 6.44 for $Y_3Al_5O_{12}$ [19]. It is clear that the ET from the matrix to Eu^{3+} is not involved in the excitation of the ions, since the band gap is far from the energy levels of the Eu^{3+} ions and no evidence of the defect states have been found. Thus, we suggest that the charge transfer (CT) transition or direct excitation of

Eu^{3+} ions, by f–d transition is responsible for efficient Eu^{3+} excitation in the case of Al_2O_3 and $Y_3Al_5O_{12}$ matrix. Moreover, since the absorption of the matrices is close to zero in the investigated range and the recombination of the ion itself does not depend on the excitation wavelength, the PLE spectra therefore correspond directly to the excitation efficiency of the Eu^{3+} ions.

The proposed mechanism responsible for the main excitation band is a direct f–d transition. The theory proposed by Nakazawa [20] makes it possible to establish the energy position of the lowest f–d transition, which for Eu^{3+} ion was determined as 7.94 eV (156 nm). Unfortunately, this result lies outside the scope of our investigation here, but certainly it is not the source of the observed excitation bands.

In the high-energy part of the optical spectra of f-compounds, not only f–d but also CT transitions give raise to strong absorption bands. The CT follows the transition of the electron from 2p full orbit O^{2-}, which energetically belongs to the top of the valence band, to a charge transfer state (CTS) of the trivalent RE ion, resulting in RE transition to a divalent form. As a result, the CT appears as an intense and wide band in absorption, and excitation spectra due to a spin and dipole allowed transition [21]. The stimulated emission process is not reversible. The Eu^{3+} ions are joined to the matrix, thus the electron comes back from CT state to its initial ion by transferring its energy to the Eu^{3+}. Eu^{3+} is stimulated to the ^5D_J ($J = 0, 1$) state from which the intra 4f orbital emission takes place. As was shown by Carnall [22], f–d and CT bands may largely overlap and their assignment is quite difficult and even impossible without the help of calculations. However, based on the Jørgensen formula [23], CT energy relative to the Eu^{3+} ground state in oxides is expected to be ca. 5.39 eV ($\lambda \approx 230$ nm). Among the lanthanide series, Eu^{3+} and Yb^{3+} have the highest optical electronegativity, thus much lower CT state due to the higher electron affinity of f^6 and f^{13} electronic configurations. In the more advanced Nakazawa approach [20], the established transition energy takes into account many electron effects and, for the O^{2-}–Eu^{3+} charge transfer excitation, the energy was calculated as corresponding to 227 nm. However, both estimated values of the charge transfer energy are far away from our measured values.

To explain the difference in the CT energy for the investigated matrices, the environment of the ions has to be taken into account. It has been already shown that the CT absorption band position depends on the covalence of matrix bonds. Hoefdraad [25] reported that the longer the bond length of Eu ligand, the longer the wavelength of the CT band position. Also other possible factors, i.e. the covalence or ionicity, the coordinate number, the potential field of the coordinate ions, the standard cation oxidation potential were identified as the factors influencing the position of the CT band [26]. As a result, the charge transfer position is sensitive to the ion environment and it can vary from matrix to matrix over a broad range. Dorenbos [27] showed that possible CT energy is in the range from 3.3 to 6.5 eV. The empirical formula proposed by Ling Li et al. [26] describes the relationship between CT energies and environmental factors, based on the dielectric theory of complex crystals. They introduced and calculated the environmental factor (h_e) for many crystal matrices to describe their influence on the optical properties of Eu^{3+} ions. For example, h_e of $Y_3Al_5O_{12}$ is equal to 0.733 and the related CT energy is 5.54 eV (223 nm). However, this environmental factor is established for the fully crystallized $Y_3Al_5O_{12}$ matrix, where all the Eu^{3+} ions usually occupy the dodecahedral *c* site with D_2 symmetry [6]. In our case, the sol-gel matrices are in the amorphous phase. Thus, Eu^{3+} ions are substituted at many sites in the host materials, which leads to much broader charge transfer bands, which are red shifted in the PLE spectra, because of the weaker chemical bond Eu^{3+}–O^{2-}, compared with the crystallized matrix. The values of the CT energies obtained from PLE spectra of Al_2O_3:Eu^{3+} and $Y_3Al_5O_{12}$ are 4.98 eV and 4.75 eV, respectively. As we expected, the observed CT energy for $Y_3Al_5O_{12}$ is slightly lower than the CT energy in crystallized matrix (5.54 eV) [26].To the best of our knowledge, the CT energy in Al_2O_3 crystal has not been determined so far. Finally, the CT is considered to be responsible for the efficient excitation mechanism of the Eu^{3+} ions in all the investigated matrices.

CT states influence the emission properties of Eu^{3+} ions as well. The closer the CT state is to the 4f orbitals, the more intensive the spin-orbit interaction between them and the more intensive the emission related to electric dipole transition. This expectation is in good agreement with our samples containing the Al_2O_3 and $Y_3Al_5O_{12}$ matrices. The first matrix has higher CT energy (4.98 eV) and lower intensity of the $^5D_0$–$^7F_2$ transition (1.0 a.u.). For the latter matrix, the CT state is closer to 4f orbitals (4.75 eV) and higher intensity of the $^5D_0$–$^7F_2$ transition (12.8 a.u.) is observed.

To fully characterize the properties of our samples required for the phosphorous material, the photoluminescence lifetimes were measured. PL delay related to the $^5D_0$–$^7F_2$ (at 615 nm) transitions were observed for both samples, which were excited by the wavelength of the maximum of the excitation band, i.e. 249 and 260 nm for Al_2O_3 and $Y_3Al_5O_{12}$, respectively. The decay time of the Eu^{3+} ions depends mainly on the surrounding crystal field, and can change in a wide range, from several microseconds to milliseconds, when the ions are doped in various host materials (i.e. 4.0 ms for $Y_3Al_5O_{12}$) [28]. However, photoluminescence lifetime depends also on the excitation mechanism and non-radiative processes. Dai et al. [29] showed also that Eu^{3+} photoluminescence lifetime depends strongly on the ion concentration and he observed an exponential decrease from 162 to 32 μs. This decrease was attributed to the increase in the non-radiative relaxation rates due to the cross relaxation process among the Eu^{3+} ions. This decrease was more significant for the ions in the surrounding with more defected state. Knowing that our samples are in amorphous phase and the doping concentration is relatively high (30%), we expected that the observed photoluminescence lifetime would be relatively short. Figure 3 shows the PL decay for our samples with fitted theoretical curves. For both the samples, a fast recombination process with $t = 10$ μs was observed, however, the intrinsic properties of the setup were found to be the cause of it. For samples with Al_2O_3 and $Y_3Al_5O_{12}$ matrices, long lifetimes were determined as $\tau_{1CT} = 120$ μs and $\tau_{2CT} = 328$ μs. The discovered lifetimes confirm previous results, stating that the smaller CT energy, the stronger the interaction of the CT state with 4f orbitals and the higher the observed PL intensity in the steady-state condition, which are related to the long lifetime emission.

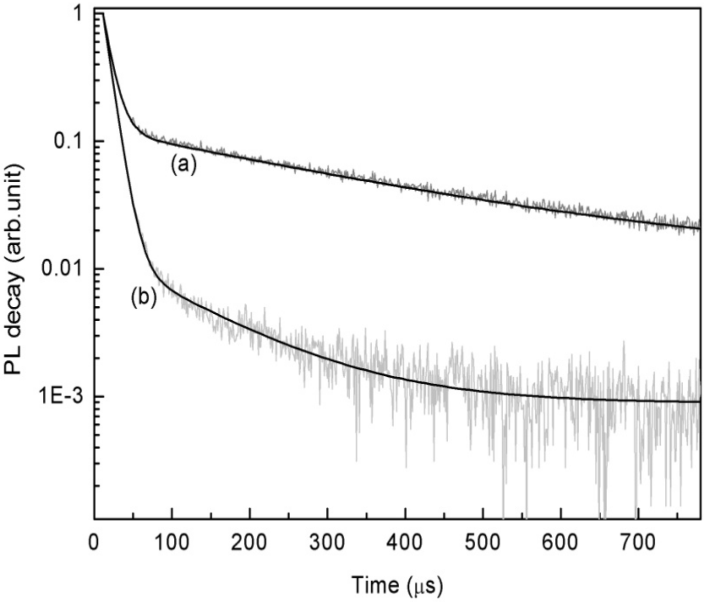

Fig. 3. PL decay spectra of $^5D_0$–$^7F_2$ transition in $Y_3Al_5O_{12}$:Eu^{3+} (a) and Al_2O_3:Eu^{3+} (b) samples excited at the maximum of PLE spectra (260 and 249 nm, respectively)

In Table 1, the PL and PLE intensity data have been summarized and compared with the reciprocal of the ESS parameter, the CT position and the photoluminescence lifetime. The agreement between the values of these parameters and the theory was found, which asserts that the efficiency of rare earth ion excitation increases as the centrosymmetricity of the ion environment decreases.

Table 1. PL, PLE intensities, ESS^{-1} parameter, CT position and photo-luminescence lifetime

Sample	PL [a.u.]	PLE [a.u.]	ESS^{-1}	CT [eV]	τ_{PL} [μs]
Al_2O_3:Eu^{3+}	1	1	6	4.98	120
$Y_3Al_5O_{12}$:Eu^{3+}	12.4	12.4	86	4.75	328

4. Conclusions

Eu^{3+} ions doped into an amorphous host material were proved to be effective light emitters. The samples were fabricated using the inexpensive sol-gel technology in conjunction with a low-cost after-treatment process. In the investigations, the f–f transitions were observed to be responsible for the intensive PL emission of Eu^{3+} ions in any matrix. The ESS parameter was determined to describe the influence of the crystal field on the emission of Eu^{3+} ions in the amorphous matrix. It was found that the broad excitation band related to CT is responsible for efficient ion excitation, which gives us more flexibility in inducing efficient Eu^{3+} excitation. The knowledge of the origin of the excitation mechanism is important because various excitation mechanisms undergo different quenching processes, which can be optimized to influence the efficiency of the emitters.

Acknowledgement

The authors would like to thank to N.V. Gaponenko and G. K. Maliarevich from the Belarusian State University of Informatics and Radioelectronics (Minsk, Belarus) for the delivered samples. Moreover, one of the authors (A.P.) acknowledges financial support from the from fellowship co-financed by European Union within the European Social Fund and financial support from the Foundation for Polish Science within the START programme.

References

[1] KIM T., YOON Y., HWANG Y., CHUNG H., KIM I.H., AHN Y., Mater. Lett., 47 (2001), 290.
[2] MOLCHAN I.S., GAPONENKO N.V., KUDRAWIEC R., MISIEWICZ J., THOMPSON G.E., Mater. Sci. Eng. B, 105 (2003), 37.
[3] KUDRAWIEC R., MISIEWICZ J., BRYJA L., MOLCHAN I.S., GAPONENKO N.V., J Alloys Compd., 341 (2002), 211.
[4] WITTMANN H.F., GRUNER J., FRIEND R.H., SPENCER G.W.C., MORATTI S.C., HOLMES A.B., Adv. Mater., 7 (1995), 541.
[5] KENYON A.J., Prog. Quant. Electron., 26 (2002), 225.
[6] RAVICHADRAN D., ROY E., CHAKHOVSKOI A.G., HUNT C.E., WHITE W.B., ERDEI S., J. Lumin., 71 (1997), 291.
[7] MAEDA N., WADA N., ONODA H., MAEGAWA A., KOJIM K., Opt. Mater., 27 (2005), 1851.
[8] MALIAREVICH G.K., GAPONENKO N.V., MUDRYI A.V., DROZDOV Y.N., STEPIKHOVA M.V., STEPANOVA E.A., Semiconductors, 43 (2009), 158.
[9] MOLCHAN I.S., GAPONENKO N.V., KUDRAWIEC R., MISIEWICZ J., BRYJA L., THOMPSON G.E., SKELDON P., J. Alloys. Compd., 341 (2002), 251.
[10] MOLCHAN I.S., GAPONENKO N.V., KUDRAWIEC R., MISIEWICZ J., THOMPSON G.E., SKELDON P., J. Electrochem. Soc., 151 (2004), H16.
[11] GAPONENKO N.V., MOLCHAN I.S., SERGEEV O.V., THOMPSON G.E., PAKES A., SKELDON P., KUDRAWIEC R., BRYJA L., MISIEWICZ J., PIVIN J.C., HAMILTON B., STEPANOVA E.A., J. Electrochem. Soc., 149 (2002), H49.
[12] WALSH B.M., *Judd–Ofelt Theory: Principles and Practices*, [In:] B. di Bartolo, O. Forte (Eds.), *Advances in Spectroscopy for Lasers and Sensing*, Springer, New York, 2006, p. 403.
[13] BUNZLI J.-C.G., *Rare Earth Luminescence Centres in Organic and Biochemical Compounds*, [In:] G. Liu, B. Jacquier (Eds.), *Spectroscopic Properties of Rare Earths in Optical Materials*, Springer, New York, 2005, p. 462.
[14] HARADA M., GOTO M., J. Alloys. Compd., 408–412 (2006), 1193.
[15] PENG A., XIE E., JIA C., JIANG R., LIN H., Mater. Lett., 59 (2005), 3866.
[16] ZHAO Z., ZENGA Q.G., ZHANGA Z.M., DING Z.J., J. Lumin., 122 (2007), 862.
[17] ZHU Y., DING C., J. Solid State. Chem., 139 (1998), 124.
[18] SHIIKI K., IGARASHI M., KAIJYU H., Jpn. J. Appl. Phys., 42 (2003), 5185.

[19] XU Y.N., CHING W.Y., Phys. Rev. B, 59 (1999), 10530.

[20] NAKAZAWA E., J. Lumin., 100 (2002). 89.

[21] YU O., LIU Y., WU S., LU X., HUANG X., LI X., J. Rare Earth, 26 (2008), 783.

[22] CARNALL W.T., J. Less Common Met., 122 (1986), 1.

[23] KRUPA J.C., J. Solid State Chem., 178 (2005), 483.

[24] YAVETSKIY R., DUBOVIK M., TOLMACHEV A., TARASOV V., Phys. Stat. Sol. (c), 2 (2005), 268.

[25] HOEFDRAAD H.E., J. Solid State Chem., 15 (1975), 175.

[26] LI L., ZHANG S., J. Phys. Chem. B, 110 (2006), 21438.

[27] DORENBOIS P., J. Phys-Condens. Mater., 15 (2003), 8417.

[28] CHEN X.Y., LIU G.K., J. Solid State Chem., 178 (2005), 419.

[29] DAI Q., SONG H., WANG M., BAI X., DONG B., QIN R., QU X., ZHANG H., J. Phys. Chem. C, 112 (2008), 19399.

Received 10 August 2009